H. Moreno, Phys. Rev. Letters 25, 625 (1970).

[7]H. Gemmel and H. A. Kastrup, Nucl. Phys. B14, 566 (1969); H. Gemmel and H. A. Kastrup, Z. Physik 229, 321 (1969).

[8]One should not expect the model to be accurate at small momentum transfers, since in that kinematical region the deflection might be due to several (not necessarily just one) very soft collisions. This may lead to "double counting" and it was pointed out by Professor R. Blankenbecler.

[9]In previous papers (Ref. 6), the field has been assumed to be massive, neutral, and of vector character. In this paper, two possibilities are explored: (a) scalar mesons and (b) vector mesons. One can then compare the two cases easily and, furthermore, find in the vector-meson case the results of the first paper of Ref. 6 for the elastic form factors in a generalized form for inelastic nucleon-resonance processes.

[10]R. P. Feynman, Phys. Rev. Letters 23, 1415 (1969); in *High Energy Collisions*, Third International Conference held at State University of New York, Stony Brook, 1969, edited by C. N. Yang *et al.* (Gordon and Breach, New York, 1969), p. 237.

[11]F. Bloch and A. Nordsieck, Phys. Rev. 52, 54 (1937); D. Yennie, S. Frautschi, and H. Suura, Ann. Phys. (N.Y.) 13, 379 (1961).

[12]See first and last papers of Ref. 6.

[13]After subtraction of terms of the same type as W_f in Eq. (7), which may be defined to be zero with the operational procedure of Eq. (8). That procedure defines the ambiguous product of the two δ functions of the same argument as the limit of the product of the two δ functions where one of them has its argument infinitesimally displaced. But then products of the type $\delta(k^2-\mu^2)\delta(k\cdot p)$ are zero since both k and p are timelike and $k\cdot p \neq 0$.

[14]The variable

$$1+\frac{Q^2}{m'^2}=\rho'=\frac{\omega'}{\omega'-1}=\frac{p\cdot(p+2q)}{(p+q)^2}$$

with $\omega'=\omega+m^2/Q^2$ was studied in Ref. 3, where it was shown to originate in a natural way in the parton model. It was suggested by the work of G. Cocho and J. Salazar, Phys. Rev. Letters 27, 892 (1971).

[15]S. D. Drell and T.-M. Yan, Phys. Rev. Letters 24, 181 (1970); G. West, *ibid.* 24, 1206 (1970). See also the last paper of Ref. 6.

[16]Bars on the symbols that appeared in the scalar-meson calculation will denote the same quantities in the vector-meson case.

[17]In the rest frame of the nucleon, $E_{p+q}=\nu+m$ ($p\cdot q=m\nu$); $m'=[(p+q)^2]^{1/2}=[m^2+2m\nu(1-x)]^{1/2}$, $x=Q^2/2m\nu$. Therefore, if $m\tau\sim(m'/m)^{\epsilon-1}$, $\epsilon>0$, then

$$t_{\text{life}}=(E_{p+q})(\tau/m')$$
$$\cong m^{-1}(1+\nu/m)[1+2\nu(1-x)/m]^{\epsilon/2-1},$$

which will be large in the Bjorken limit $\nu\to\infty$, x fixed.

PHYSICAL REVIEW D VOLUME 5, NUMBER 6 15 MARCH 1972

Normalization of the $\pi\pi$ Veneziano Model Using a Multiperipheral Model with π, K, and ω Exchange*

L. A. P. Balázs† and V. V. Dixit
Department of Physics, Purdue University, Lafayette, Indiana 47907
(Received 3 September 1971)

We consider a model of the Amati-Bertocchi-Fubini-Stanghellini-Tonin (ABFST) type with ω and K exchange, in addition to the usual pion exchange. Instead of using the usual formalism, we sum the ABFST $\pi\pi\to\pi\pi$ graphs approximately by projecting out into crossed-channel partial waves (which can be continued to unphysical angular momenta) and constructing a diagonal Padé approximant. This satisfies unitarity exactly in the elastic region of that channel. In practice only the [1, 1] approximant was considered. The relevant graphs are then built up from $\pi\pi\to\pi\pi$, $\pi\pi\to\pi\omega$, and $\pi\pi\to K\bar{K}$ input kernels, each of which is approximated by Veneziano-model resonances with a cutoff at the mass of the $J=3$ resonance and with off-shell effects neglected. By requiring that there be an output pole at $t\simeq 0$ in the unphysical $I=1$, $J=\frac{1}{2}\pi\pi$ state and that its residue be consistent with the one predicted by the $\pi\pi$ Veneziano model, we can determine the normalization coefficient $\bar{\beta}$ of that model. We obtain $\bar{\beta}=0.65$, which corresponds to a ρ width of 135 MeV.

I. INTRODUCTION

Although the Veneziano model,[1] or for that matter any dual amplitude, is capable of giving successful predictions for the ratios of resonance widths in any given problem, it does not say anything about their absolute values. In other words, the over-all normalization of the Veneziano amplitude is arbitrary. To determine it, one has to turn to some kind of dynamical model. One such model is the multiperipheral integral equation, which can be either of the multi-Regge[2] or the Amati-Bertocchi-Fubini-Stanghellini-Tonin (ABFST) type.[3] It has recently been argued that

the former is highly suspect, since it depends on the use of Regge behavior down to fairly low energies.[4] The latter, on the other hand, seems to lead to output Regge trajectories which are too low, at least when simple pion-pole dominance is assumed.[5] One way of removing this difficulty is to include the effect of other exchanges.[6]

In the present model we shall explicitly include K and ω exchange in addition to π exchange. These are, of course, only the lightest among the particles which could come in. However, most of the others are either Regge recurrences or lie on exchange-degenerate trajectories, and it is usually a reasonable approximation to replace a Regge trajectory by the lightest particle lying on it, at least for the sort of application we shall be concerned with. The actual graphs of the model are then constructed in terms of the resonances given by the Veneziano model. This involves the Veneziano model for other processes besides $\pi\pi$ scattering, and the normalization for these will either be determined from experiment or related to the $\pi\pi$ normalization through SU(3) symmetry. The $\pi\pi$ normalization itself will be determined by requiring consistency between the output $\pi\pi$ trajectory and the corresponding input Veneziano trajectory in the neighborhood of $t=0$.

The output $\pi\pi$ trajectory is calculated by following the usual procedure of summing the $\pi\pi$ scattering graphs which arise when the multiperipheral production amplitudes are inserted into a multiparticle unitarity relation. In Sec. II we discuss a Padé-approximant technique for approximately carrying out this sum. We first make a partial-wave projection in the t channel, and continue the resulting amplitude to unphysical angular momenta. We then rearrange the graphs in terms of diagonal Padé approximants, which satisfy unitarity exactly in the elastic region.[7] In practice we do not go beyond the [1, 1] approximant, which only involves singly peripheral graphs. The explicit construction of the input kernels for these graphs in terms of the Veneziano resonances for $\pi\pi \to \pi\pi$, $\pi\pi \to \pi\omega$, and $\pi\pi \to K\bar{K}$ is given in Sec. III.

In Sec. IV we carry out an approximate evaluation of our graphs in the $J=\frac{1}{2}$ unphysical state. To avoid any Pomeranchuk complications, we only consider the $I=1$ state. If our output Regge trajectory is to be consistent with the input $\pi\pi$ Veneziano trajectory, we must then have a pole at $t\cong 0$, the point at which the multiperipheral model is most likely to be valid anyway. The requirement that the input and output parameters of this pole be consistent with each other enables us to determine the Veneziano normalization. In principle this also determines the intercept of the trajectory. One of our graphs requires a cutoff, however, which is needed to prevent a divergence and to guarantee that the squared momentum transfers in the peripheral chain are not much larger than 1 GeV^2. We will therefore *fix* the input intercept at $\alpha=\frac{1}{2}$ [which, as we shall see, is required by partial conservation of axial-vector current (PCAC) in the $\pi\pi$ Veneziano model], and simply adjust the cutoff parameter so that the output intercept is the same. The resulting cutoff is in fact of the right order of magnitude.

Finally, in Sec. V we discuss a multichannel Padé technique in which several processes are described simultaneously. The diagonal approximants, which are now matrices, then satisfy a coupled-channel unitarity relation.

II. PADÉ-APPROXIMANT SUMMATION OF ABFST GRAPHS

The model for production from two incident pions which we shall use is illustrated in Fig. 1, where all the produced particles are taken to be pions or kaons. The effect of the latter will turn out to be small, although its inclusion does improve our result somewhat. This is consistent with the experimentally observed fact that the large majority of produced particles are pions. Of course, this fact does not prevent us from having unstable particles such as the ω among the vertical lines of Fig. 1. But such a diagram would be dual to a similar diagram in which these lines are all pions, and so we would be double-counting if we included them explicitly.

For the exchanged (horizontal) lines, we shall take the π, K, and ω, which give the poles lying closest to the forward direction. If we now insert

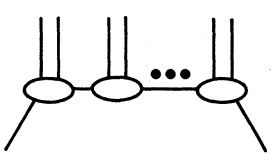

FIG. 1. Diagram for an ABFST production amplitude. The horizontal lines can represent π, K, and ω exchange.

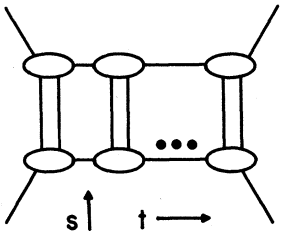

FIG. 2. Multiperipheral contribution to the four-point amplitude.

the diagrams of Fig. 1 into a multiparticle unitarity relation, the resulting absorptive part of the $\pi\pi$ scattering amplitude is given by a sum of graphs of the type shown in Fig. 2. If we insert this into a fixed-momentum-transfer dispersion relation we obtain the corresponding amplitude, which is also given by Fig. 2. The input kernels V_s out of which these graphs are then constructed are given by Fig. 3 and the corresponding contribution to the invariant amplitude can be written as

$$V(s,t)=\frac{1}{\pi}\int ds'\,\frac{V_s(s',t)}{s'-s}\,, \tag{1}$$

where s, t, and u are the usual Mandelstam variables. We have dropped the u channel for the time being, but will restore it later. In the case where all the lines represent pions, for example, $V_s(s,t)$ is just the elastic absorptive part and is given by

$$V_s(s,t)=\frac{q}{4\pi\sqrt{s}}\int d\Omega\, T^*(s,t_1)T(s,t_2)\,, \tag{2}$$

where T is the amplitude describing the blobs of Fig. 3, q is the magnitude of the three-momentum, and t_1 and t_2 are the squares of the momentum transfers between the intermediate and final and the initial and intermediate states, respectively. At $t=0$, V_s is simply related to the elastic cross section.

The graphs of Fig. 2 are usually summed by using either the ABFST integral equation for the absorptive part[3] or the Bethe-Salpeter equation for the full amplitude.[8] We shall, instead, use Padé approximants, which are much simpler. These have already seen considerable application in other areas of elementary-particle physics[7,9] and so we shall not dwell on their more detailed properties here. We first make a partial-wave projection of the graphs of Fig. 2 in the t channel, and make the usual Froissart-Gribov continuation to unphysical J. We then associate a parameter λ with each kernel of the type shown in Fig. 3, so that the graphs of Fig. 2 give an expansion for the partial-wave amplitude of the form

$$T_J(t)=\lambda T_J^1+\lambda^2 T_J^2+\cdots, \tag{3}$$

which we normalize such that $T_J=(\sqrt{t}/q)e^{i\delta}\sin\delta$ in the elastic region, where q is the c.m. momentum in the t channel and δ is the phase shift. We will set $\lambda=1$ at the end of the calculation.

The diagonal $[N,N]$ Padé approximant is now defined by

$$[N,N]=\frac{\lambda n_J^1+\cdots+\lambda^N n_J^N}{1+\lambda d_J^1+\cdots+\lambda^N d_J^N}\,, \tag{4}$$

where the coefficients n_J^i and d_J^i are chosen in such a way that an expansion of Eq. (4) in powers of λ agrees with the expansion (3) up to the λ^{2N} term. A diagonal approximant like Eq. (4) can be easily shown to satisfy unitarity exactly in the elastic region of the t channel.[7] In the case of nonrelativistic potential scattering it has also been shown to converge to the correct amplitude for large enough N.[7] In practice, however, we have only considered the $[1,1]$ approximant. This gives an approximate amplitude

$$T_J(t)\simeq\frac{T_J^1}{1-T_J^2/T_J^1}\,, \tag{5}$$

where we have set $\lambda=1$ and where T_J^1 is the partial-wave projection of Eqs. (1) and (2). In the t-channel isospin state $I=1$, which does not have any Pomeranchuk complications and which we shall consider from now on, T_J^2 is given by the graphs of Fig. 4. We therefore have only singly peripheral graphs contributing explicitly to this order of approximation. A pole in T_J will now occur at $t=t_J$ when

$$1/T_J(t_J)=0\,. \tag{6}$$

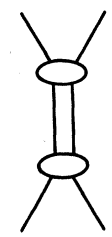

FIG. 3. A typical input kernel out of which the graphs of Fig. 2 are built.

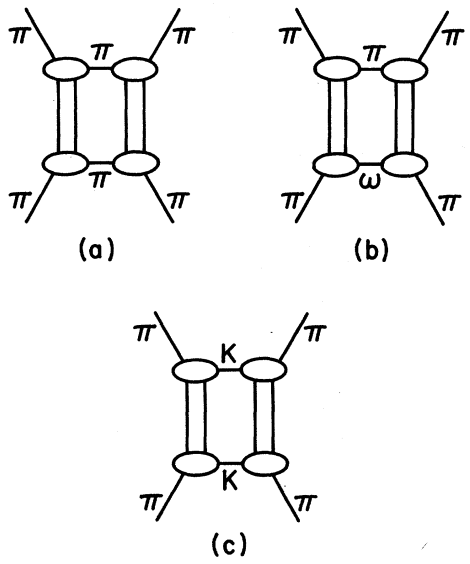

FIG. 4. Graphs which contribute to the function T_J^2 of Secs. II–IV.

The corresponding residue γ_J is

$$\gamma_J = -\left(\frac{\partial}{\partial t}\frac{1}{T_J(t)}\right)^{-1}_{t=t_J}, \tag{7}$$

and the equation for a Regge trajectory $\alpha(t)$ is given by

$$J = \alpha(t_J). \tag{8}$$

III. CONSTRUCTION OF INPUT KERNELS

The graphs of Fig. 4 involve three kinds of input kernels, corresponding to Fig. 3 for the processes $\pi\pi \to \pi\pi$, $\pi\omega \to \pi\pi$, and $\pi K \to \pi K$. The first is also the one which gives T_J^1. Now in evaluating the graphs of Fig. 4, we require off-shell expressions for these kernels. For this we shall follow the usual procedure of approximating $V_s(s,t)$ by its on-shell value[3,5] and calculating V itself from Eq. (1). This procedure is the one which is favored if we invoke a "criterion of maximal convergence."[6]

We have already seen that only $\pi\pi$ or πK intermediate states should come into Fig. 3. Since the ρ and f^0 decay almost totally into $\pi\pi$ and the $K^*(892)$ almost totally into πK, and since these are the dominant low-energy resonances, we have

$$V_s(s,t) \simeq T_s(s,t) \tag{9}$$

at low energies, where T_s is the corresponding full absorptive part for the process considered. We will use Eq. (9) up to the g meson for $\pi\pi \to \pi\pi$ and $\pi\omega \to \pi\pi$ and the $J=3$ Regge recurrence of the $K^*(892)$ for $\pi K \to \pi K$. Actually, it is not clear whether this is quite correct, since these resonances may decay predominantly into other channels and so should probably be suppressed. We will include them to compensate for higher-s contributions which we are neglecting.[5] Explicit estimates made by Chew, Rogers, and Snider[4] have shown that such a neglect is justified.

To evaluate $T_s(s,t)$ we use the Veneziano model. For $\pi\pi \to \pi\pi$ the corresponding amplitude is

$$T^\pi(s,t) = 2\bar{\beta}_\pi[F(\alpha(t),\alpha(s)) - F(\alpha(t),\alpha(u))] \tag{10}$$

in the t-channel $I=1$ state, with

$$F(x,y) = -\frac{\Gamma(1-x)\Gamma(1-y)}{\Gamma(1-x-y)} \tag{11}$$

and $\alpha(s) = \alpha_0 + \alpha' s$. Equation (10) gives the usual Regge asymptotic behavior with a residue function

$$\frac{b}{\pi} = 2\frac{\alpha'^{\alpha}}{\Gamma(\alpha)}\bar{\beta}_\pi. \tag{12}$$

This can be related to the γ_J function of Eq. (7) through

$$\gamma_\alpha = \frac{\sqrt{\pi}}{4\alpha'}\frac{\Gamma(\alpha+1)}{\Gamma(\alpha+\frac{3}{2})}\frac{b}{\pi}. \tag{13}$$

For $\pi\omega \to \pi\pi$ we have a T matrix

$$M = T^\omega(s,t)\epsilon_{\mu\nu\rho\sigma}e_\mu p_{1\nu}p_{2\rho}p_{3\sigma}, \tag{14}$$

where e_μ is the ω polarization vector and the p_i are the pion momenta. The invariant amplitude T^ω is given by

$$\begin{aligned} T^\omega(s,t) = \bar{\beta}_\omega[&B(1-\alpha(t),1-\alpha(s)) \\ &+ B(1-\alpha(t),1-\alpha(u)) \\ &+ B(1-\alpha(s),1-\alpha(u))], \end{aligned} \tag{15}$$

where $\alpha(s)$ is the same as for $\pi\pi \to \pi\pi$ and B is the Euler B function. Finally, for $\pi K \to \pi K$, which becomes $\pi\pi \to K\bar{K}$ in the t channel, we have

$$T^K(s,t) = 2\bar{\beta}_K[F(\bar{\alpha}(t),\bar{\alpha}(s)) - F(\bar{\alpha}(t),\bar{\alpha}(u))], \tag{16}$$

where F is again given by Eq. (11) and $\bar{\alpha}(s) = \bar{\alpha}_0 + \alpha' s$ is the K^* trajectory. If we take the absorptive part of Eqs. (10), (15), and (16) in the s variable and use Eq. (9), we obtain in each case an expression of the form

$$V_s^i(s,t) = \sum_{n=1}^{3} V_n^i(t)\delta(s - s_n^i), \tag{17}$$

where the $V_n^i(t)$ are polynomials in t, the s_n^i are the positions of the resonances, and $i = \pi, \omega, K$, respectively.

We will determine our trajectory parameters in the usual way[10] by imposing the PCAC conditions $\alpha(m_\pi^2) = \frac{1}{2}$ and $\bar{\alpha}(m_K^2) = \frac{1}{2}$, and requiring $\alpha(s)$ to give the correct experimental value for the ρ mass. This gives $\alpha_0 \simeq 0.5$, $\bar{\alpha}_0 \simeq 0.28$, and $\alpha' = \frac{1}{60}$ in pion mass units; we are taking α' to be the same for both $\alpha(s)$ and $\bar{\alpha}(s)$, an assumption which is approximately consistent with the experimental K^* mass. The parameter $\bar{\beta}_\omega$ was determined in terms of the ρ residue in the $\pi\pi \to \pi\omega$ process, which gives $\bar{\beta}_\omega = \alpha' g_{\rho\pi\pi}g_{\rho\pi\omega}/4\pi$. Now $g_{\rho\pi\pi}{}^2 \propto \Gamma_\rho$ and $g_{\rho\pi\omega}{}^2 \propto \Gamma_\omega/\Gamma_\rho$ if we assume the Gell-Mann–Sharp–Wagner model,[11] where Γ_ρ and Γ_ω are widths of the ρ and ω resonances. Thus $\bar{\beta}_\omega$ depends only on Γ_ω. If we take the experimental value $\Gamma_\omega = 12$ MeV, we obtain $g_{\rho\pi\pi}g_{\rho\pi\omega}/4\pi = 0.458$. The constant $\bar{\beta}_K$ in Eq. (15) was also determined in terms of the ρ residue and is given by $\bar{\beta}_K = g_{\rho\pi\pi}g_{\rho KK}/4\pi$. Since the same procedure applied to Eq. (11) gives $\bar{\beta}_\pi = g_{\rho\pi\pi}{}^2/4\pi$ and since SU(3) gives[12] $2g_{\rho KK}{}^2 = g_{\rho\pi\pi}{}^2$ we thus have $\bar{\beta}_K = (\frac{1}{2})^{1/2}\bar{\beta}_\pi$. The value of $\bar{\beta}_\pi$ itself will be determined self-consistently.

If we insert Eq. (17) into Eq. (1) we have

$$V^i(s,t) = \frac{1}{\pi}\sum_{n=1}^{3}\frac{V_n^i(t)}{s_n^i - s}. \tag{18}$$

Now $V^i(s,t)$ is needed only for $s<0$ within any of our equations and in the $I=1$ state all the terms in the summation of Eq. (18) are positive there, at

least for $t \approx 0$. We can therefore make the further approximation of replacing $V^i(s, t)$ by a single effective pole

$$V^i(s, t) = \frac{c^i(t)}{s_R^i - s}, \tag{19}$$

where

$$c^i(t) = \frac{1}{\pi} \sum_{n=1}^{3} V_n^i(t) \tag{20}$$

and

$$s_R^i = \frac{\pi c^i(t)}{\sum_{n=1}^{3} [V_n^i(t)/s_n^i]}. \tag{21}$$

Equation (19) then reproduces Eq. (18) exactly at $s = 0$ and $s = \infty$ and to within several percent for all other negative values of s.

IV. SELF-CONSISTENT DETERMINATION OF $\bar{\beta}$

Our remaining problem is now to evaluate the diagrams of Fig. 4 in the appropriate angular momentum state or states, insert them into Eq. (5), and require the output trajectory as calculated from Eqs. (6)–(8) to be consistent with the one in Eq. (11). Since the multiperipheral model is presumably most reliable near $t = 0$ and since the $t = 0$ intercept of the latter trajectory is $\alpha_0 = 0.5$, we would therefore be interested in using Eq. (5) in the neighborhood of $J = \frac{1}{2}$. Now there is more than one way in which $\bar{\beta}$ could be calculated self-consistently. The procedure we found most convenient was to do the entire calculation at $J = \frac{1}{2}$ and require Eq. (6) to be satisfied with $t_J = 0$. Then $\bar{\beta}$ was varied until Eq. (7) gave the same value of γ_J as Eqs. (13) and (12).

In practice, a Logunov-Tavkhelidze-Blankenbecler-Sugar (LTBS) type of approximation[13] was used to evaluate Figs. 4(a) and 4(c). In this approximation the product of the propagators for the two horizontal lines is replaced by a more tractable function. In a given partial wave we then have contributions

$$T_J^{2(i)}(t) = \frac{1}{2\pi} \int_0^\infty \frac{d\nu'}{\nu' - \nu_i} \left(\frac{\nu'}{\nu' + m_i^2} \right)^{1/2} |V_J^{(i)}(\nu', \nu_\pi, t)|^2, \tag{22}$$

where $i = \pi, K$ for Figs. 4(a) and 4(c), respectively; $\nu_i = q_i^2 = \frac{1}{4}t - m_i^2$; and $m_\pi = 1$ and m_K are the pion and kaon masses. The V_J is a partial-wave projection of Eq. (19) and is given by

$$V_J^i(p'^2, p^2, t) = \frac{c^i(t)}{p'p} Q_J \left(\frac{s_R^i + p'^2 + p^2}{2p'p} \right), \tag{23}$$

where we have included an extra factor of 2 to take into account the effect of the u channel. It turns out to be reasonable to make an asymptotic approximation for Q_J,

$$Q_J(x) \simeq \frac{\sqrt{\pi}\,\Gamma(J+1)}{(2x)^{J+1}\Gamma(J+\frac{3}{2})}. \tag{24}$$

With this approximation, the integral of Eq. (22) can be evaluated analytically for $J = \frac{1}{2}$.

Figure 4(b) is somewhat messy to evaluate by means of the above approximation, mainly because of the fact that the intermediate particles in the t channel have unequal masses. We shall, instead, use the fact that the partial-wave projection of Fig. 4(b) has a right-hand cut and a left-hand cut in the t plane. Actually, for general J it is more convenient to deal, not with the projection $T_J^{2(\omega)}$ itself but, rather, with the function $\nu_\pi^{-J} T_J^{2(\omega)}$ which has better analyticity properties. Now the left-hand cut is relatively far from the region of interest and so our approximation will be to drop it. We then have

$$\nu_\pi^{-J} T_J^{2(\omega)}(t) = \frac{1}{\pi} \int_{(m_\omega+1)^2}^{\Lambda} \frac{dt'}{t' - t} q_\omega'^{2J+1} \sqrt{t'} |W_J^\omega(t', t)|^2, \tag{25}$$

where

$$W_J^\omega(t', t) = \frac{c^\omega(t)[J(J+1)]^{1/2}}{(q_\pi' q_\omega')^J (2J+1)} [Q_{J-1}(a) - Q_{J+1}(a)],$$

$$a = [s_R^\omega + \tfrac{1}{2}(t' - m_\omega^2 - 3)]/(2q_\pi' q_\omega'), \tag{26}$$

$$q_\omega'^2 = \frac{1}{4t'}(m_\omega^2 - 1 + t')^2 - m_\omega^2,$$

and $q_\pi'^2 = \frac{1}{4}t' - 1$. The cutoff Λ was put in to prevent a divergence of the integral and guarantees that the squared momentum transfers t_i in the peripheral chain are bounded by $|t_i| \lesssim \Lambda$. The original multiperipheral assumption is that these $|t_i|$ are not much larger than $1\,\mathrm{GeV}^2$.[4] The cutoff can also be thought of as a rough way of parametrizing the more-distant singularities. As before we shall make the asymptotic approximation (24) for $Q_{J-1}(a)$ and drop $Q_{J+1}(a)$, which is of the same order as the higher-order terms in an expansion of $Q_{J-1}(a)$. The integral of Eq. (25) can then be done exactly for $J = \frac{1}{2}$.

The above expressions enable us to determine the Padé approximant (5) in which

$$T_J^1(t) = V_J^\pi(\nu_\pi, \nu_\pi, t), \tag{27}$$

where V_J^π is given by Eq. (23), and

$$T_J^2(t) = \sum_{i = \pi, \omega, K} T_J^{2(i)}(t), \tag{28}$$

with the $T_J^{2(i)}$ given by Eqs. (22) and (25). The value of Λ in the latter integral was adjusted so that Eq. (6) was satisfied with $t_J = 0$ for $J = \frac{1}{2}$. This, as we have seen, guarantees that the output ρ tra-

jectory has the correct intercept. The output $\gamma_{1/2}^{\text{out}}$ was then calculated from Eq. (7) for various input values of $\bar{\beta}_\pi$, until it was equal to the value $\gamma_{1/2}^{\text{in}}$ as given by Eqs. (13) and (12). This finally occurred for $\bar{\beta}=0.65$ which corresponds to a ρ width of 135 MeV in the Veneziano model of Eq. (10). (Experimentally the ρ width is about 125 MeV, so $\bar{\beta}\approx 0.6$.) The corresponding value of the cutoff was $\Lambda=75.3$ (1.476 GeV^2) which is roughly consistent with the value of 1 GeV^2 required by the original assumptions of peripheralism. Our self-consistency condition appears to be a fairly stable one, since $\gamma_{1/2}^{\text{out}}/\gamma_{1/2}^{\text{in}}$ deviates sufficiently rapidly from unity as $\bar{\beta}_\pi$ is varied from the self-consistency value. For example, with $\bar{\beta}_\pi=0.60$ we have $\gamma_{1/2}^{\text{out}}/\gamma_{1/2}^{\text{in}}=1.06$, while $\bar{\beta}_\pi=0.68$ gives $\gamma_{1/2}^{\text{out}}/\gamma_{1/2}^{\text{in}}=0.96$.

Our result is also not too sensitive to the cutoff. Suppose, for example, we decrease Λ by 5%, but leave all the other input parameters unchanged. Then, of course, the input and output trajectories are no longer the same. With $\gamma_{1/2}^{\text{out}}=\gamma_{1/2}^{\text{in}}$, Eq. (6) gives $t_{1/2}=2.14$, which corresponds to an output intercept $\alpha_0\simeq 0.46$ while the value of $\bar{\beta}_\pi$ changes to $\bar{\beta}_\pi=0.62$ (a 4% change). But since we do wish to have a self-consistent intercept, and since this intercept is, after all, fixed at $\alpha_0\simeq 0.5$ by PCAC in our model, perhaps a more meaningful way of seeing how sensitive our results are to the cutoff is to change Λ but at the same time adjust $g_{\rho\pi\omega}{}^2$ so that the output intercept continues to be the same. With $\Lambda=71.6$ (a 5% decrease) we then have $(g_{\rho\pi\omega}{}^2/4\pi)=0.472$, whereas with $\Lambda=79.1$ (a 5% increase) we have $(g_{\rho\pi\omega}{}^2/4\pi)=0.304$, which should be compared with the value $(g_{\rho\pi\omega}{}^2/4\pi)=0.373$ in the original calculation (with $\Lambda=75.3$). On the other hand, $\bar{\beta}_\pi$ in each case differs by less than 0.5% from the original value $\bar{\beta}_\pi=0.65$. This also shows that $\bar{\beta}_\pi$ is extremely insensitive to $g_{\rho\pi\omega}{}^2$.

V. MATRIX PADÉ-APPROXIMANT SUMMATION OF MULTIPERIPHERAL GRAPHS

We shall now discuss an improved, but somewhat more complicated, way of using Padé approximants to sum multiperipheral graphs with more than one exchange, which amounts to a different way of rearranging the expansion (3). For simplicity, we shall ignore the K meson, although its inclusion would be straightforward. We shall also confine ourselves again to the $I=1$ state. Then, instead of considering Fig. 2 with only pions for the external lines, we consider the coupled-channel problem in which the $\pi\pi\to\pi\pi$, $\pi\pi\to\pi\omega$, $\pi\omega\to\pi\pi$, and $\pi\omega\to\pi\omega$ processes are treated simultaneously. The corresponding amplitudes $T_{J(11)}$, $T_{J(12)}$, $T_{J(21)}$, and $T_{J(22)}$ would then be written in the usual way as elements of a 2×2 matrix

$$T_J=\begin{pmatrix} T_{J(11)} & T_{J(12)} \\ T_{J(21)} & T_{J(22)} \end{pmatrix} \tag{29}$$

and would each be described by graphs of the type shown in Fig. 2. According to the arguments of Sec. II all the vertical intermediate lines are again pions.

The rest of the procedure is exactly the same as in Sec. II. We again have Eqs. (3), (4), and (5), except that the various terms are now 2×2 matrices. The condition for a pole will be given by

$$\det T_J{}^{-1}(t_J)=0 \tag{30}$$

instead of Eq. (6), however, and the corresponding residue by

$$(\gamma_J)_{ij}=-\text{cof}\,[T_J{}^{-1}(t_J)]_{ij}\Big/\left[\frac{d}{dt}\det T_J{}^{-1}(t)\right]_{t=t_J} \tag{31}$$

(where "cof" means "cofactor") instead of Eq. (7). A diagonal Padé approximant will now satisfy the two-channel form of unitarity, at least below the $\omega\pi\pi$ threshold – the [1, 1] approximant actually satisfies it for all t. In this respect, the matrix approximant is an improvement over the one in Sec. II, which only satisfies simple $\pi\pi$ elastic unitarity, and, while not ignoring the $\pi\omega$ intermediate state, treats it in a less satisfactory manner. On the other hand, the matrix version is considerably more complicated. The $T_J{}^2$ term in the [1, 1] approximant (5), for example, would involve the graphs of Fig. 5 in addition to Figs. 4(a) and 4(b). These graphs, which are also of the singly peripheral type, are discussed further in the Appendix.

In conclusion, it should be mentioned that the

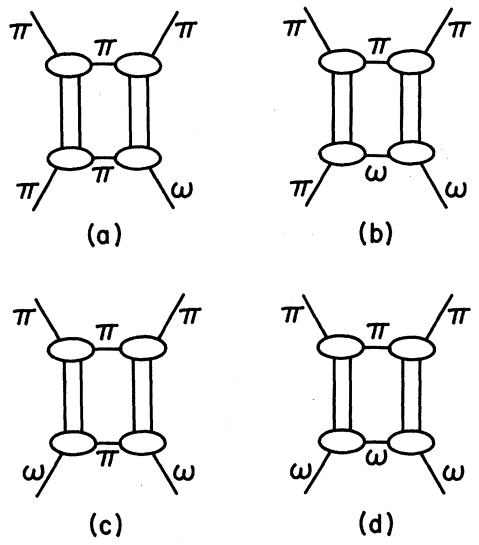

FIG. 5. Additional graphs which would contribute to T_J^2 in the matrix version of Sec. V.

Padé technique, whether of the simple variety used in Secs. II–IV or the multichannel form discussed above, is by no means restricted to the simple type of multiperipheral model which we have been considering. For example, it would be straightforward, if not altogether simple, to consider a model in which the horizontal lines are Reggeized. Equations (3)–(5) would continue to be used but the expressions for T_J^i would, of course, be different. It is also not essential to use partial-wave amplitudes. At $t=0$, for instance, we could, instead, use an $O(4)$ expansion in terms of Gegenbauer polynomials. The simple connection with t-channel unitarity would be lost, however.

ACKNOWLEDGMENTS

The authors would like to thank S. Mahajan for several helpful discussions. One of us (L.A.P.B.) would also like to thank Professor S. Treiman and Dr. N. Goldwasser for their hospitality at the National Accelerator Laboratory, where part of this paper was written.

APPENDIX

The graphs of Fig. 5 can be evaluated approximately by means of techniques very similar to those used in Sec. IV. The LTBS approximation is again fairly simple to use for Figs. 5(a) and 5(c), where the particles corresponding to the horizontal lines have equal mass. Thus Fig. 5(b) gives a contribution to the $\pi\pi \to \pi\omega$ partial wave of

$$T^{\pi}_{J(12)} = \frac{1}{2\pi}\int_0^{\infty} \frac{d\nu'}{\nu' - \nu_\pi}\left(\frac{\nu'}{\nu' + m_\pi^2}\right)^{1/2} \times V^{\omega}_J(\nu', q_\omega^2, t) V^{\pi}_J(\nu', \nu_\pi, t), \quad \text{(A1)}$$

where

$$q_\omega^2 = \frac{1}{4t}(m_\omega^2 - 1 + t)^2 - m_\omega^2,$$

T_J is normalized so that $T_J = (S-1)/(q_\pi q_\omega)^{1/2}$, S being the appropriate element of the partial-wave S matrix; V^{π}_J is given by Eq. (23), and V^{ω}_J by

$$V^{\omega}_J(p'^2, p^2, t) = c^{\omega}(t)\frac{[J(J+1)]^{1/2}}{2J+1}[Q_{J-1}(b) - Q_{J+1}(b)], \quad \text{(A2)}$$

with

$$b = \frac{1}{2p'p}\left(s_R^{\omega} - \frac{(m_\omega^2 - m_\pi^2)^2}{4t} + p'^2 + p^2\right). \quad \text{(A3)}$$

In $\pi\omega \to \pi\omega$ scattering the ρ trajectory contributes only to states with $L = J$. For such states Fig. 5(c) gives a contribution

$$T^{\pi}_{J(22)} = \frac{1}{2\pi}\int_0^{\infty} \frac{d\nu'}{\nu' - \nu_\pi}\left(\frac{\nu'}{\nu' + m_\pi^2}\right)^{1/2} |V^{\omega}_J(\nu', q_\omega^2, t)|^2, \quad \text{(A4)}$$

where V^{ω}_J is again given by Eq. (A2) and the normalization is such that $T_J = (S-1)/q_\omega\sqrt{t}$, where S is the appropriate element of the partial-wave S matrix.

Figures 5(b) and 5(d) involve an input kernel with Fig. 3 corresponding to the process $\pi\omega \to \pi\omega$. The Veneziano model for this process is difficult to write down[14] and so we shall content ourselves with the contribution of the ρ, although it would be straightforward to include a higher resonance like the g. The prescription for going off the mass shell would again be to first evaluate an on-shell value for V_s and then use Eq. (1) to evaluate the contribution of the kernel to the corresponding invariant amplitude. There is more than one invariant amplitude involved in this case.[15]

Since the horizontal lines in Figs. 5(b) and 5(d) have unequal masses, the LTBS approximation again becomes complicated to use. If, instead, we follow the procedure applied to Fig. 4(b), we obtain the contribution

$$T^{\omega}_{J(12)} = \frac{(q_\pi q_\omega)^J}{\pi}\int_{(m_\omega+1)^2}^{\infty} \frac{dt'}{t' - t} q_\omega'^{2J+1}\sqrt{t'}\, W^{\omega}_J(t', t) U_J(t', t), \quad \text{(A5)}$$

where the amplitude is normalized in the same way as in Eq. (A1); W^{ω}_J is given by Eq. (26); and

$$U_J(t', t) = -\frac{1}{4}\frac{g_{\rho\pi\omega}^2}{4\pi}\frac{1}{t' q_\omega'^2}\left(\frac{E^2 - k^2\cos\bar{\theta}}{2J+1}[Q_{J+1}(c) - Q_{J-1}(c)] + q_\omega'^{-2}[k^4\sin^2\bar{\theta} + k^2(E^2 + \overline{W}^2)\cos\bar{\theta} + 2k^2 E\overline{W}]Q_J(c)\right), \quad \text{(A6)}$$

with

$$k^2 = \frac{1}{4t}(m_\omega^2 - m_\pi^2 + t)^2 - m_\omega^2,$$

$$\cos\bar{\theta} = 1 + \frac{1}{2k^2}[2(m_\omega^2 + m_\pi^2) - t - m_\rho^2],$$

$$c = \frac{1}{2q_\omega'^2}[m_\rho^2 - 2(m_\omega^2 + m_\pi^2) + t'] - 1,$$

$$E^2 = m_\pi^2 + k^2, \quad \text{and} \quad \overline{W}^2 = m_\omega^2 + k^2.$$

Similarly Fig. 4(d) gives a contribution

$$T^{\omega}_{J(22)} = \frac{q_\omega^{2J}}{\pi}\int_{(m_\omega+1)^2}^{\infty}\frac{dt'}{t'-t}q_\omega'^{2J+1}\sqrt{t'}\,|U(t',t)|^2 . \tag{A7}$$

Needless to say, although Figs. 4(a), 5(a), and 5(c) could be evaluated quite readily by the LTBS approximation, they could also be evaluated by the technique of the preceding paragraph. This then gives contributions

$$T^{2(\pi)}_{J} = \frac{\nu_\pi^{J}}{\pi}\int_4^{\infty}\frac{dt'}{t'-t}\frac{|V_J^{(\pi)}(q_\pi'^2, q_\pi'^2, t)|^2}{q_\pi'^{2J-1}\sqrt{t'}}, \tag{A8}$$

$$T^{\pi}_{J(12)} = \frac{(q_\pi q_\omega)^J}{\pi} \times\int_4^{\infty}\frac{dt'}{t'-t}\frac{V_J^{(\pi)}(q_\pi'^2, q_\pi'^2, t)V_J^{\omega}(q_\pi'^2, q_\omega'^2, t)}{q_\pi'^{J-1}q_\omega'^{J}\sqrt{t'}}, \tag{A9}$$

and

$$T^{\pi}_{J(22)} = \frac{q_\omega^{2J}}{\pi}\int_4^{\infty}\frac{dt'}{t'-t}q_\pi'\frac{|V_J^{\omega}(q_\pi'^2; q_\omega'^2, t)|^2}{q_\omega'^{2J}\sqrt{t'}} \tag{A10}$$

instead of Eqs. (22), (A1), and (A4). The latter equations are probably more accurate.

*Work supported in part by the U. S. Atomic Energy Commission.

†Work supported in part from an Alfred P. Sloan Foundation Fellowship.

[1]G. Veneziano, Nuovo Cimento 57, 190 (1968).

[2]G. F. Chew and A. Pignotti, Phys. Rev. 176, 2112 (1968); G. F. Chew, M. L. Goldberger, and F. E. Low, Phys. Rev. Letters 22, 208 (1969); I. G. Halliday, Nuovo Cimento 60A, 177 (1969); I. G. Halliday and L. M. Saunders, *ibid.* 60A, 494 (1969); L. Caneschi and A. Pignotti, Phys. Rev. 180, 1525 (1969); 184, 1915 (1969); G. F. Chew and W. R. Frazer, *ibid.* 181, 1914 (1969); J. S. Ball and G. Marchesini, *ibid.* 188, 2209 (1969).

[3]L. Bertocchi, S. Fubini, and M. Tonin, Nuovo Cimento 25, 626 (1962); D. Amati, A. Stanghellini, and S. Fubini, *ibid.* 26, 896 (1962).

[4]G. F. Chew, T. Rogers, and D. R. Snider, Phys. Rev. D 2, 765 (1970).

[5]D. M. Tow, Phys. Rev. D 2, 154 (1970).

[6]A crude way of doing this was used by L. A. P. Balázs, Phys. Rev. D 4, 1117 (1971).

[7]For a recent review of the properties of Padé approximants and some of their applications to elementary-particle physics, see J. Zinn-Justin, Phys. Reports 1C, 55 (1971).

[8]J. S. Ball and G. Marchesini, Phys. Rev. 188, 2508 (1969).

[9]S. T. Chiang, UCLA Ph.D. thesis (unpublished).

[10]C. Lovelace, Phys. Letters 28B, 264 (1968).

[11]M. Gell-Mann, D. Sharp, and W. D. Wagner, Phys. Rev. Letters 8, 261 (1962).

[12]See, for example, R. H. Capps, Phys. Rev. Letters 10, 312 (1963).

[13]A. A. Logunov and A. N. Tavkhelidze, Nuovo Cimento 29, 380 (1963); R. Blankenbecler and R. Sugar, Phys. Rev. 142, 1051 (1966).

[14]P. Carruthers and E. Lasley, Phys. Rev. D 1, 1204 (1970).

[15]See, for instance, K. Kang, Phys. Rev. 140, B1626 (1965).

PHYSICAL REVIEW D VOLUME 5, NUMBER 6 15 MARCH 1972

Operator Formulation of a Dual Multiparticle Theory with Nonlinear Trajectories*

Darryl D. Coon
University of Pittsburgh, Pittsburgh, Pennsylvania 15213

and

S. Yu and M. Baker
University of Washington, Seattle, Washington 98195

(Received 6 December 1971)

An operator formalism for a dual-resonance theory with nonlinear trajectories is presented and an explicit, factorized operator representation is obtained for the N-point function. Operator Ward identities are also given.

In a previous paper,[1] we considered a meromorphic dual N-point Born term B_N with poles at energies $= s_l^{1/2}$ given by

$$1+(1-q)(a+bs_l) = q^{-l} . \tag{1}$$

a and b are constants and q is a parameter between zero and unity whose value determines the degree of nonlinearity of the trajectories.[2] In the limit $q \to 1$, the trajectories become linear and $B_N \to V_N$, the Veneziano N-point amplitude.[3]